

Energy of the quasi-free electron in low density Ar and Kr: Extension of the local Wigner-Seitz model

Xianbo Shi ^{a,b}, Luxi Li ^{a,b}, Gina Moriarty ^a, C.M. Evans ^{a,b,*},
G.L. Findley ^c

^a*Department of Chemistry and Biochemistry, Queens College – CUNY, Flushing,
NY 11367, United States*

^b*Department of Chemistry, Graduate Center – CUNY, New York, NY 10016,
United States*

^c*Department of Chemistry, University of Louisiana at Monroe, Monroe, LA
71209, United States*

Abstract

We present new measurements of the perturber induced shift of the CH₃I ionization energy at low perturber number densities and analyze these data within the local Wigner-Seitz model previously used at high density. We compare the local Wigner-Seitz model with the scattering approach developed by Fermi, and modified by Alekseev and Sobel'man, and show that the local Wigner-Seitz model extends smoothly into the low density region and accurately predicts the temperature dependence of the shift in ionization energy.

Key words: Wigner-Seitz model, Fermi model, field ionization, quasi-free electron energy, electron mobility

1 Introduction

The interaction of high- n dopant Rydberg states with perturbing atoms or molecules has been investigated at low perturber densities (cf. Fig. 1, open markers) [1–7] and at high perturber densities (cf. Fig. 1, closed markers) [8–15]. In both regions, the perturber-induced energy shift $\Delta(\rho_P)$, where ρ_P is the perturber number density, of a high- n dopant Rydberg state (or of the dopant ionization energy) is assumed to be separable into (i) the interaction of the optical electron with the perturber, and (ii) the interaction of the dopant core with the perturber. However, the modeling of these interactions has been approached differently in the two density regions. At low perturber densities, the dopant core/perturber interaction is treated statistically while the optical electron/perturber interaction is handled via scattering theory. At high densities, both interactions are determined within a statistical mechanical model, although the scattering of the optical electron by the perturber is also included. The transition between these two density regions has not been experimentally investigated to our knowledge, although it is crucial to understanding the relationship between the low density and high density models.

In this paper we present the perturber-induced shift $\Delta(\rho_P)$ of the CH₃I ioniza-

* Corresponding author.

Email addresses: `xshi@gc.cuny.edu` (Xianbo Shi), `lli1@gc.cuny.edu` (Luxi Li), `cherice.evans@qc.cuny.edu` (C.M. Evans), `findley@ulm.edu` (G.L. Findley).

tion energy, determined from field ionization of CH₃I high- n Rydberg states, in the low to medium density regime (i.e., $\rho_P \leq 3 \times 10^{21} \text{ cm}^{-3}$) for the perturbers argon and krypton. Using these data we show that our recently developed local Wigner-Seitz model [10–15] extends smoothly into the low density region and accurately predicts the temperature dependence of $\Delta(\rho_P)$. We also show that the empirically determined constant in the local Wigner-Seitz model [10–15] is equivalent to a phase shift arising from the electron/perturber interaction.

2 Experimental

Field ionization measurements were performed with monochromatized synchrotron radiation [7] having a resolution of 0.9 Å (or 8 meV in the spectral region of interest). The details of the experimental cell and of the determination of a field ionization spectrum from photoionization measurements have been given elsewhere [10]. Field ionization spectra were energy corrected [10] for the effects of both the low and high field. The low field F_L and high field F_H were adjusted to optimize the field ionization spectrum at each perturber number density, with $F_L = 830 - 2,500 \text{ V cm}^{-1}$ and $F_H = 2,500 - 6,700 \text{ V cm}^{-1}$. The total error range for any experimental point is given by a sum of the field correction error, the goodness-of-fit error (for fitting a field ionization spectrum to a gaussian lineshape), and the error arising from the energy uncertainty due to the resolution of the monochromator (i.e., $\pm 4 \text{ meV}$). This total error averages to $\pm 0.010 \text{ eV}$ for all measurements presented here.

CH₃I (Aldrich, 99.45%), argon (Matheson Gas Products, 99.9999%), and krypton (Matheson Gas Products, 99.998%) were used without further purification. Absorption and photoionization spectra were measured for CH₃I (0.1 mbar)

to verify the absence of impurities. The number densities of both argon and krypton were calculated from the Strobridge equation of state [16] using a standard iterative technique with an estimated error of $\pm 0.2\%$ of the calculated number density [17,18]. (The coefficients for the Strobridge equation of state for argon and krypton were obtained from Gosman et al. [17] and from Street and Staveley [18], respectively.) The gas handling system and the procedures used to ensure homogeneous mixing of dopant and perturber have been described previously [7]. Prior to the introduction of the dopant, the experimental cell and gas handling system were baked to a base pressure of low 10^{-8} Torr, and in order to ensure no perturber contamination by the dopant (which was present at a concentration of < 100 ppm), the gas handling system was allowed to return to the low 10^{-7} Torr range before the addition of the perturber. Cross contamination between perturbers was prevented by baking the gas handling system until the pressure was in the low 10^{-8} Torr range before introducing a new perturber.

3 Results and Discussion

At low perturber number densities, a dopant Rydberg state shifts in energy and the transition lineshape broadens as a result of collisional interactions. For high- n dopant Rydberg states (or for the dopant ionization energy), one can assume that the dopant core/perturber and optical electron/perturber interactions are separable. Following Fermi [1], the perturber-induced shift $\Delta(\rho_{\text{P}})$ of the dopant ionization energy is then given by

$$\Delta(\rho_{\text{P}}) = \Delta_{sc}(\rho_{\text{P}}) + \Delta_{pol}(\rho_{\text{P}}) , \quad (1)$$

where $\Delta_{sc}(\rho_P)$ is the shift resulting from scattering of the optical electron off of the perturber, and $\Delta_{pol}(\rho_P)$ is the shift due to the polarization of the perturber by the dopant core.

For high- n Rydberg states, the optical electron is loosely bound and can therefore be considered quasi-free. Moreover, near threshold the kinetic energy of the optical electron is approximately zero, and the scattering of the optical electron by a perturber is predominantly s -wave. Averaging this scattering interaction over the total number of perturber atoms yields [1,3]

$$\Delta_{sc}(\rho_P) = \frac{2\pi\hbar^2}{m_e} a \rho_P , \quad (2)$$

where m_e is the electron mass, \hbar is the reduced Planck constant, and a is the zero-kinetic-energy electron scattering length for the perturber (which may be either positive or negative depending on the nature of the perturber).

The calculation of the polarization shift $\Delta_{pol}(\rho_P)$ assumes that the dopant core polarizes all of the perturber atoms within the orbit of the Rydberg electron, or [1,2]

$$\Delta_{pol}(\rho_P) = -\frac{\alpha_P}{2} \sum_i^N F_i(R_i)^2 , \quad (3)$$

where α_P is the polarizability of the perturber, $F_i(R_i)$ is the field at the position of the i th perturber due to the dopant core, R_i is the distance between the i th perturber and the dopant core, and N is the number of perturbors within the orbit of the Rydberg electron. For non-interacting perturbors $F_i(R_i) = e/R_i^2$, and since F_i is a short-ranged interaction, the sum in eq. (3) can be converted to an integral over all perturbors [1–5]:

$$\Delta_{pol}(\rho_P) = -\frac{\alpha_P e^2}{2} (4\pi\rho_P) \int_{R_1}^{\infty} \frac{R^2}{R^4} dR = -2\pi\alpha_P e^2 \rho_P \frac{1}{R_1} , \quad (4)$$

where R_1 is a cut-off radius. Assuming that this cut-off radius is the Weisskopf

impact radius for core/perturber scattering, namely [3,19]

$$r_W = \left(\frac{\pi \alpha_P e^2}{4 \hbar v} \right)^{1/3},$$

where v is the thermal velocity of the perturbers, gives [4–6]

$$\Delta_{pol}(\rho_P) = -(32\pi^2)^{1/3} (\alpha_P e^2)^{2/3} (\hbar v)^{1/3} \rho_P \approx -6.81 (\alpha_P e^2)^{2/3} (\hbar v)^{1/3} \rho_P. \quad (5)$$

(We should note here that Alekseev and Sobel'man [3,19] have provided a formal treatment of $\Delta_{pol}(\rho_P)$ within the impact approximation of line broadening theory that yields an equation similar to eq. (5), but with a scale factor of 6.21 instead of 6.81.) Eqs. (2) and (5), however, are expected to fail at high perturber number densities, since the assumption of non-interacting perturbers is not valid in this density regime.

At high perturber number densities, the separability of the electron/perturber and dopant core/perturber interactions remains valid, and therefore the perturber-induced energy shift $\Delta(\rho_P)$ can still be written as a sum of interactions [9–15]

$$\Delta(\rho_P) = P_+(\rho_P) + V_0(\rho_P), \quad (6)$$

where $P_+(\rho_P)$ is the (adiabatic) ensemble average dopant core/perturber polarization energy arising from the perturber distribution about the neutral dopant [20], and $V_0(\rho_P)$ is the quasi-free electron energy in the perturber medium. $V_0(\rho_P)$ is given by [8,10–15]

$$V_0(\rho_P) = \frac{3}{2} k_B T + E_k(\rho_P) + P_-(\rho_P), \quad (7)$$

where $3k_B T/2$ ($k_B \equiv$ Boltzmann constant) is the thermal energy of the quasi-free electron, $E_k(\rho_P)$ is the zero-point kinetic energy of the quasi-free electron, and $P_-(\rho_P)$ is the ensemble average electron/perturber polarization energy. The polarization energies $P_{\pm}(\rho_P)$ can be calculated from a standard statistical

mechanical treatment, via [10–15]

$$P_{\pm}(\rho_P) = -4\pi\rho_P \int_0^{\infty} g(r) w_{\pm}(r) r^2 dr . \quad (8)$$

In this equation, $g(r)$ is the radial distribution function appropriate for the interaction, and $w_{\pm}(r)$ is an interaction potential having the form [10–15,21]

$$w_{\pm}(r) = -\frac{1}{2}\alpha e^2 \sum_i^N r_i^{-4} f_{\pm}(r_i) , \quad (9)$$

with $f_{\pm}(r)$ being a screening function that incorporates the repulsive interactions between the induced dipoles in the perturbing medium. In eq. (8), $g(r) = g_{\text{PD}}(r)$, where $g_{\text{PD}}(r)$ is the (neutral) dopant/perturber radial distribution function, for the calculation of $P_{+}(\rho_P)$, while $g(r) = g_{\text{PP}}(r)$, where $g_{\text{PP}}(r)$ is the perturber/perturber radial distribution function, for the calculation of $P_{-}(\rho_P)$. It is important to note, however, that since $f_{+}(r)$ incorporates induced dipole interactions in the perturbing medium, $g_{\text{PP}}(r)$ is also involved in the determination of $P_{+}(\rho_P)$.

The Schrödinger equation for the zero-point energy of the quasi-free electron in a dense perturber is [8,10–15]

$$\nabla^2\psi + \frac{2m_e}{\hbar^2} \left(V_0 - \frac{3}{2}k_B T - V(r) \right) \psi = 0 , \quad (10)$$

where $V(r)$ is the spherically symmetric potential that describes the interaction between the quasi-free electron and the neat perturber. The local Wigner-Seitz model [10–15] assumes that $V(r) = P_{-}(\rho_P) + V_{loc}(r)$, where $P_{-}(\rho_P)$ is given by eq. (8) and is a constant for any given density, and $V_{loc}(r)$ is a short-ranged potential which accounts for local dynamic polarization of a perturber by the optical electron. Within these assumptions, eq. (10) can be rewritten

as

$$\nabla^2 \psi + \frac{2m_e}{\hbar^2} (E_k - V_{loc}(r)) \psi = 0 . \quad (11)$$

If we define a wavevector $k_0 \equiv 2m_e E_k / \hbar^2$, then for a low-kinetic-energy (i.e., *s*-wave) electron scattering elastically from the short-ranged potential, the asymptotic solution is [22]

$$\psi(r) \sim \frac{1}{r} \sin(k_0 r + \eta_0) , \quad (12)$$

where η_0 is the phase shift induced by the short-ranged potential.

At high densities, the minimum distance between the optical electron and a single perturber is given by the absolute value of the scattering length $|a|$. However, the maximum distance for the short-ranged interaction is determined by the average translational symmetry for the problem. In a neat fluid of interacting perturbers the density is nonuniform, with the local density $\rho_P(r)$ given by [23,24] $\rho_P(r) = \rho_P g_{PP}(r)$. Using this local density, the Wigner-Seitz radius that determines the average translational symmetry is [10–15]

$$r_\ell \equiv \sqrt[3]{\frac{3}{4\pi g_{max} \rho_P}} , \quad (13)$$

where g_{max} is the maximum of the perturber/perturber radial distribution function $g_{PP}(r)$. (The local Wigner-Seitz radius is one half of the spacing between two perturbers in the first solvent shell.) If the interactions in the first solvent shell dominate E_k , then the total range r_b for the local potential $V_{loc}(r)$ will be given by $r_b = r_\ell - |a|$, and the average translational symmetry of the potential requires that $V_{loc}(r) = V_{loc}(r + 2r_b)$. Applying this condition to the asymptotic wavefunction yields

$$\sin(k_0 r + \eta_0) = \sin[k_0(r + 2r_b) + 3\eta_0] , \quad (14)$$

Thus, the wavevector k_0 , the phase shift η_0 and the scattering length a are

related by

$$\eta_0 = m\pi - k_0(r_\ell - |a|), \quad (15)$$

or $\eta_0 = -k_0(r_\ell - |a|)$ for $m = 0$. This allows the perturber induced shift $\Delta(\rho_P)$ to be written as [15]

$$\Delta(\rho_P) = P_+(\rho_P) + P_-(\rho_P) + \frac{3}{2}k_B T + \frac{\hbar^2 \eta_0^2}{2m_e(r_\ell - |a|)^2}. \quad (16)$$

for high perturber number densities.

Fig. 1 shows the perturber induced shift $\Delta(\rho_P)$ of the CH₃I ionization energy in argon and krypton plotted as a function of perturber number density ρ_P from previous low [4–6] and high density studies [10,11]. The solid lines represent eq. (1) at a temperature of 25°C with $a = -0.82$ Å for argon and $a = -1.60$ Å for krypton. The dashed lines are eq. (16) with the same zero-kinetic-energy electron scattering length a used in eq. (1), and $\eta_0 = -0.329$ [15] for Ar and $\eta_0 = -0.133$ [15] for Kr. The radial distribution functions required for determining $P_+(\rho_P)$, $P_-(\rho_P)$ and r_ℓ in eq. (16) were computed from the coupled Percus-Yevick integro-differential equation method [10,25], with a Lennard-Jones 6-12 potential used for the perturber/perturber interactions [10] and a modified Stockmeyer potential employed for the dopant/perturber interactions [10]. Clearly, eq. (1) gives an excellent fit to the low density experimental data (open markers) at room temperature, while eq. (16) gives an excellent fit to the high density experimental data (solid markers) at all temperatures. Below, we will use the field ionization of high- n CH₃I Rydberg states to show that eq. (16) can be extended into the low density regime.

Fig. 2a presents new measurements of the argon induced shift $\Delta(\rho_{Ar})$ of the CH₃I ionization energy plotted as a function of Ar number density at several temperatures. These data show that $\Delta(\rho_P)$ increases as the temperature de-

creases. The low density model [1,3–6,19] of Fermi-Alekseev-Sobel’man model [i.e., eqs. (1), (2), and (5)], predicts a decrease in $\Delta(\rho_P)$ as the temperature decreases, since the average thermal velocity v decreases with decreasing temperature. The lines in Fig. 2a represent a local Wigner-Seitz calculation with $a = -0.82 \text{ \AA}$ and $\eta_0 = -0.329$ [15], which were the parameters used to fit the high density data in Fig. 1a to within $\pm 0.3\%$ for all temperatures. Fig. 2a clearly shows that the local Wigner-Seitz model accurately predicts the temperature behavior of $\Delta(\rho_P)$ to within the experimental error of ± 10 meV. This temperature behavior arises from the temperature dependence of $P_+(\rho_P)$ caused by variations in the dopant/perturber radial distribution function $g_{PD}(r)$. Although the temperature variation in $g_{PD}(r)$ is large, the variation in $g_{PP}(r)$ is small except near the critical temperature and density of the perturber. Thus, the quasi-free electron energy $V_0(\rho_P)$ varies with temperature only near the critical density [11–14]. Fig. 2b presents new measurements of the krypton induced shift $\Delta(\rho_{Kr})$ of the CH_3I ionization energy (solid markers) plotted as a function of Kr number density at 25°C in comparison to the local Wigner-Seitz calculation (solid line). (The parameters used in the local Wigner-Seitz calculation were the same parameters used to fit the high density experimental data of Fig. 1b to within $\pm 0.3\%$ for all temperatures, namely $a = -1.60 \text{ \AA}$ and $\eta_0 = -0.133$ [15].) Again, the local Wigner-Seitz model predicts the low density shift $\Delta(\rho_{Kr})$ to within experimental error.

Since the local Wigner-Seitz model extends smoothly into the low density region, one can begin to probe the difference between $\Delta_{pol}(\rho_P)$ and $P_+(\rho_P)$, as well as that between $\Delta_{sc}(\rho_P)$ and $V_0(\rho_P)$, as shown in Fig. 3. By neglecting the fact that the perturber/perturber interactions increase as the dopant core polarizes the perturber, the low density Fermi-Alekseev-Sobel’man model

[1,3,19] greatly underestimates the perturber-induced shift caused by dopant core/perturber interactions, as has been pointed out previously in the context of sudden and adiabatic polarization effects [27]. This underestimation of $\Delta_{pol}(\rho_P)$ is counterbalanced by the overestimation of $\Delta_{sc}(\rho_P)$, since the latter neglects the polarization of the perturber by the quasi-free electron, as well as the local density of the perturber. Thus, $\Delta_{sc}(\rho_P)$ is significantly larger than the quasi-free electron energy $V_0(\rho_P)$.

In this paper, the perturber induced shift $\Delta(\rho_P)$ of the CH₃I ionization energy, obtained from field ionization of high- n CH₃I Rydberg states, was used to extend successfully the local Wigner-Seitz model to low and medium perturber number densities. We demonstrated that the temperature dependence of $\Delta(\rho_P)$ arises from dopant/perturber interactions and, therefore, is not correctly accounted for in the low density Fermi-Alekseev-Sobel'man model [1,3,19].

Acknowledgements

The experimental measurements reported here were performed at the University of Wisconsin Synchrotron Radiation Center (NSF DMR-0537588). This work was supported by grants from the Petroleum Research Fund (45728-B6), from the Professional Staff Congress - City University of New York (60074-34 35) and from the Louisiana Board of Regents Support Fund (LEQSF(2006-09)-RD-A33).

References

- [1] E. Fermi, *Nuovo Cimento* 11 (1934) 157.
- [2] H. Margenau, W. W. Watson, *Rev. Mod. Phys.* 8 (1936) 22.
- [3] V. A. Alekseev, I. I. Sobel'man, *Zh. Eksp. Teor. Fiz.* 49 (1965) 1274. [*Sov. Phys.* - *JETP* 22 (1966) 882].
- [4] A. M. Köhler, R. Reininger, V. Saile, G. L. Findley, *Phys. Rev. A* 33 (1986) 771.
- [5] A. M. Köhler, R. Reininger, V. Saile, G. L. Findley, *Phys. Rev. A* 35 (1987) 79.
- [6] A. M. Köhler, Ph.D. Dissertation, Universität Hamburg, Hamburg, Germany, 1987, and references therein.
- [7] C. M. Evans, J. D. Scott, G. L. Findley, *Rec. Res. Dev. Chem. Phys.* 3 (2002) 351, and references therein.
- [8] B. E. Springett, J. Jortner, M. H. Cohen, *J. Chem. Phys.* 48 (1968) 2720.
- [9] A. K. Al-Omari, Ph.D. dissertation, University of Wisconsin Madison, Madison, WI, 1996, and references therein.
- [10] C. M. Evans, G. L. Findley, *Phys. Rev. A* 72 (2005) 022717.
- [11] C. M. Evans, G. L. Findley, *Chem. Phys. Lett.* 410 (2005) 242.
- [12] C. M. Evans, G. L. Findley, *J. Phys. B: At. Mol. Opt. Phys.* 38 (2005) L269.
- [13] Luxi Li, C. M. Evans, G. L. Findley, *J. Phys. Chem. A* 109 (2005) 10683.
- [14] Xianbo Shi, Luxi Li, C. M. Evans, G. L. Findley, *Chem. Phys. Lett.* 432 (2006) 62.
- [15] Xianbo Shi, Luxi Li, C. M. Evans, G. L. Findley, *Nucl. Inst. Meth. A* 582 (2007) 270.

- [16] T. R. Strobridge, Nat. Bur. Std. Tech. Note 129 (1962).
- [17] A. L. Gosman, R. D. McCarty, J. G. Hust, Nat. Bur. Std. Tech. Note 27 (1969).
- [18] W. B. Streett, L. A. K. Staveley, J. Chem. Phys. 55 (1971) 2495.
- [19] I. I. Sobel'man, L. A. Vainshtein, E. A. Yukov, Excitation of Atoms and Broadening of Spectral Lines, Springer-Verlag, Berlin, 1995.
- [20] I. Messing and J. Jortner, Chem. Phys. 24 (1977) 183.
- [21] J. Lekner, Phys. Rev. 158 (1967) 130.
- [22] H. S. W. Massey, E. H. S. Burhop, Electronic and Ionic Impact Phenomena, Vol. 1, Clarendon Press, Oxford, 1969.
- [23] P. Attard, J. Chem. Phys. 91 (1989) 3072.
- [24] P. Attard, J. Chem. Phys. 91 (1989) 3093.
- [25] E. W. Grundke, D. Henderson, R. D. Murphy, Can. J. Phys. 51 (1973) 1216.
- [26] T. F. O'Malley, Phys. Rev. 130 (1963) 1020.
- [27] A. M. Köhler, V. Saile, R. Reininger and G. L. Findley, Phys. Rev. Lett. 60 (1988) 2727; errata 61 (1988) 1327. The reader should note that the adiabatic polarization energy in this reference deviates from that given in [20]; the latter is the one adopted in the present paper.

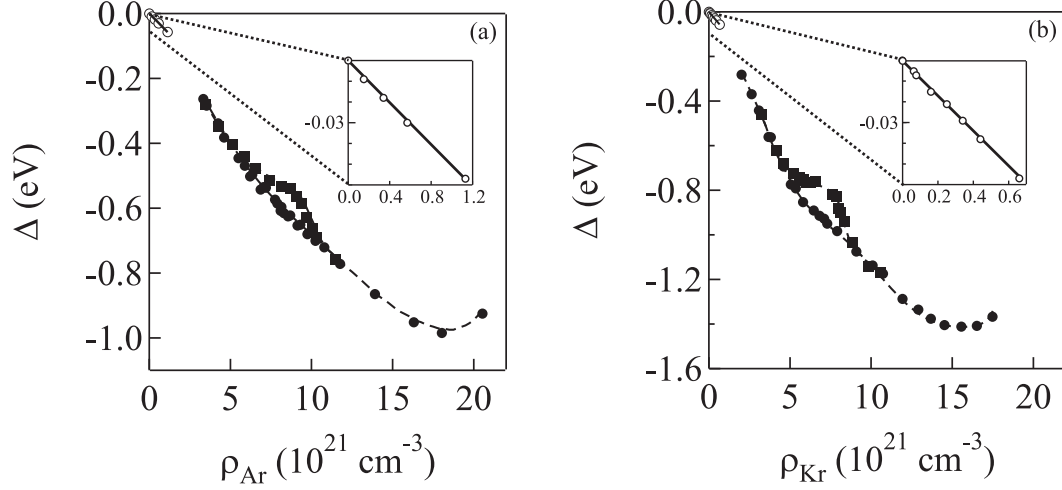


Fig. 1. The perturber induced shift $\Delta(\rho_P)$ for (a) Ar and (b) Kr plotted as a function of perturber number density ρ_P . Open markers represent experimental data [4–6] obtained from fitting room temperature photoabsorption spectra of CH_3I to the Rydberg equation. Solid markers are experimental data [10–13] obtained from field ionization of high- n CH_3I Rydberg states at various noncritical temperatures [$< 0^\circ\text{C}$] (\bullet) and on an isotherm near the critical isotherm (\blacksquare). The average error for the low density data is 10 meV, while the average error for the high density data is 15-20 meV. The solid lines are a calculation of $\Delta(\rho_P)$ using eq. (1) with $a = -0.82 \text{ \AA}$ for Ar and -1.60 \AA for Kr. The dashed lines are a calculation from eq. (16) with the parameters $a = -0.82 \text{ \AA}$ and $\eta_0 = -0.329$ for Ar [15] and $a = -1.60 \text{ \AA}$ and $\eta_0 = -0.133$ for Kr [15]. See text for discussion.

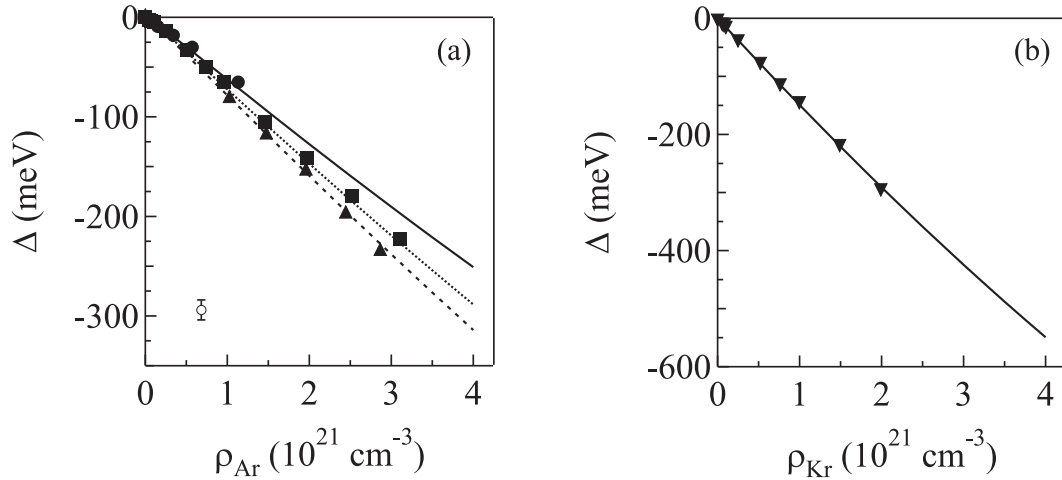


Fig. 2. The perturber-induced shift $\Delta(\rho_P)$ of the CH_3I ionization energy in (a) argon and (b) krypton plotted as a function of perturber number density ρ_P . The solid markers are the experimental data, while the lines are calculated using eq. (16). (\bullet , \blacktriangledown , solid line) 25°C , (\blacksquare , dotted line) -60°C , and (\blacktriangle , dashed line) -114°C . The potential parameters required to determine $P_{\pm}(\rho_P)$ are in Ref. [10]. For Ar [15], $a = -0.82 \text{ \AA}$ and $\eta_0 = -0.329$. For Kr [15], $a = -1.60 \text{ \AA}$ and $\eta_0 = -0.133$. The open marker is provided to show the experimental error. See text for discussion.

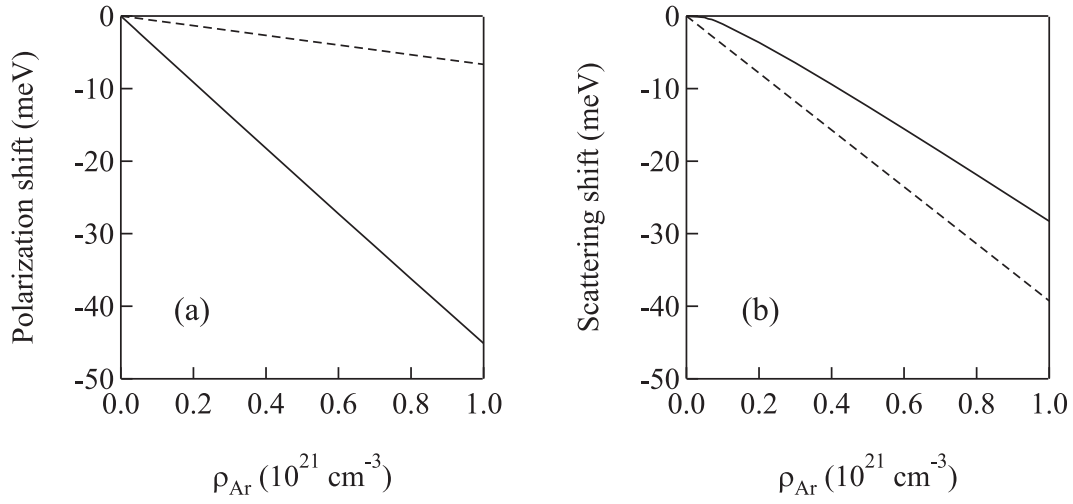


Fig. 3. (a) The argon induced shift in the CH₃I ionization energy due to CH₃I⁺/argon interactions from (solid line) the local Wigner-Seitz model [i.e., $P_+(\rho_{\text{P}})$ from eq. (8)] and from (dashed line) the Fermi-Alekseev-Sobel'man model [i.e., eq. (1)]. (b) The argon induced shift in the CH₃I ionization energy due to interaction of the optical electron with argon. (solid line) is $V_0(\rho_{\text{P}})$ calculated from eq. (7), while (dashed line) is $\Delta_{sc}(\rho_{\text{P}})$ obtained from eq. (2). All calculations were performed for a temperature of -60°C . See text for discussion.